Inorganic Chemistry

pubs.acs.org/IC Article

Electrophoresis and Biosensor-Based DNA Interaction Analysis of the First Paraben Derivatives of Spermine-Bridged Cyclotriphosphazenes

Elif Şenkuytu,* Perihan Kızılkaya, Zehra Ölçer, Uğur Pala, Derya Davarcı, Yunus Zorlu, Huriye Erdoğan, and Gönül Yenilmez Çiftçi

Cite This: https://dx.doi.org/10.1021/acs.inorgchem.9b03031

ABSTRACT: Cancer is the uncontrolled growth of abnormal cells via malignant cell division and rapid DNA replication. While DNA damaging molecules can cause cancer, their role as anticancer drugs are very significant. For this purpose, the novel series of paraben substituted spermine bridged(dispirobino) cyclotriphosphazene compounds **2**–**6** were synthesized for the first time, and their structures were characterized by various spectroscopic techniques. The solid-state structures and geometries of compounds **2**–**6** were determined using single-crystal X-ray structural analysis. In addition, it was confirmed by TGA that all compounds **1**–**6** showed high thermal stability. Two methods were used in order to investigate DNA interaction properties of the targeted molecules. While biosensor-based screening test that measures DNA hybridization efficiency on a biochip surface, the agarose gel electrophoresis method examines the effect of compounds on plasmid DNA structure. The results collected from the automated biosensor device and agarose gel electrophoresis have indicated that compounds **1**, **5**, and **6** showed higher DNA damage than the compounds **2**–**4**. According to the biosensor results, compounds **1**, **5**, and **6** showed 85%, 69%, and 77% activity, respectively.

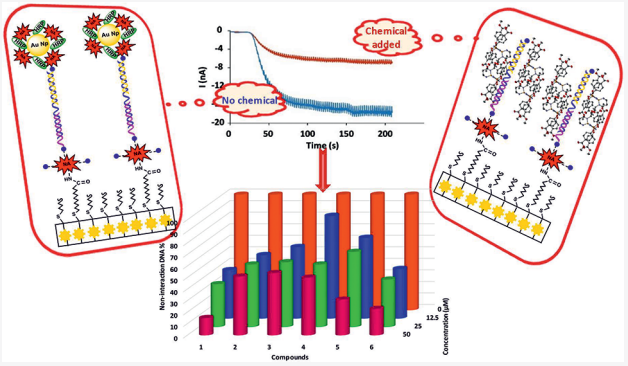

INTRODUCTION

Cancer, currently one of the most common reason for death, is caused by accumulation of several genetic mutations promoted by errors in DNA replication that eventually results in uncontrolled-malign cell formation. As cancer is mainly a DNA-based cell disorder, new-generation anticancer drugs are designed to mimic cancer. Specifically, these new generation drugs will act as DNA-damaging molecules that target cancer cell or microorganism DNAs; hence, they cause cell death or growth.[1,2] Therefore, investigation of the effects of synthesized drug candidate molecules on certain DNA is quite important to discover new drug candidates. A number of in vivo or in vitro techniques, namely electrophoresis, absorption studies, Western blot, cell growth studies, voltammetry, and spectroscopic methods, have been used to investigate DNA–drug interactions.[3−6] Biosensor-based analyses using optical and electrochemical techniques offer a good alternative in studying compound–DNA interactions due to their advantages such as speed, low cost, high sensitivity, ability to operate in turbid solutions, and possibility of miniaturization. Moreover, electrochemical biosensors enable quantitative compound–DNA interaction analysis and may give information about the strength of the interaction between the molecule and DNA.[7−9]

Natural polyamines (PA) and their biogenic derivatives found in all mammalian cells have been shown to have cytotoxic activity and important physiological roles against many human cancer cells.[10] PAs could inhibit cell growth and kill cancer cells as shown in both tissue culture and in the in vivo animal models. Additionally, they protect cells from external toxic conditions such as oxidative stress and acidic pH and against other toxic agents.[11−13] The amine functional groups have an important role in cell growth and cell proliferation, as they are involved in almost all steps of DNA, RNA, and protein synthesis. Among the amine compounds, spermine is one of the biogenic polyamines and has become an essential component in membrane stabilization, regulation of nucleic acid, and protein synthesis.[14,15] It was revealed that spermine derivatives have been shown to affect gene expression due to direct interaction of spermine with DNA. Therefore, in recent years, studies on cancer activity of

Received: October 17, 2019

https://dx.doi.org/10.1021/acs.inorgchem.9b03031
Inorg. Chem. XXXX, XXX, XXX−XXX

Scheme 1. Paraben Substituted-Dispirobino Spermine Derivative Cyclotriphosphazenes 2−6

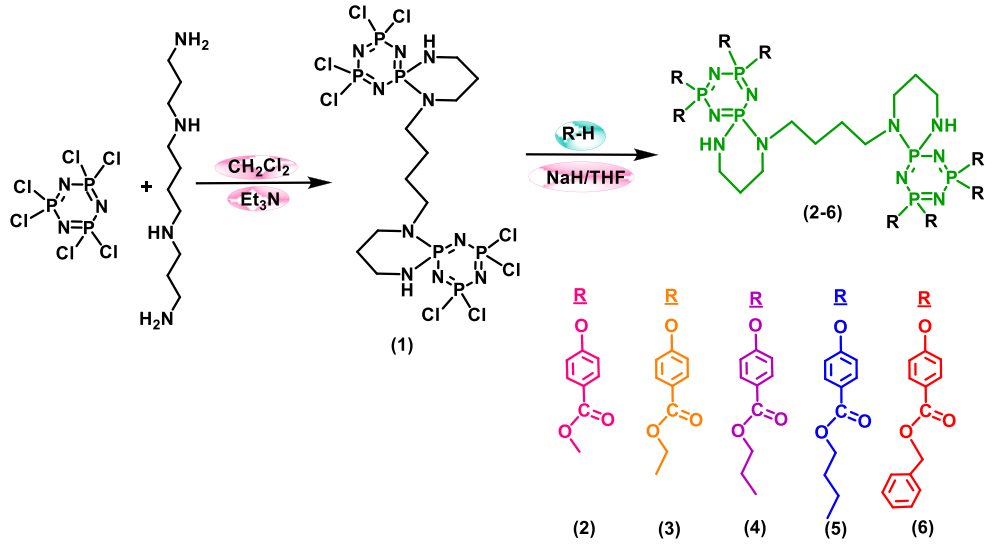

the spermine and spermine based compounds have been increased.[16,17]

Parabens are a class of compounds that have been known for nearly 100 years with their antimicrobial and antifungal properties. They consist of alkyl (methyl, ethyl, propyl, or butyl) ester compounds of *p*-hydroxybenzoic acid, and have been widely used in food, cosmetics, and the pharmaceutical industry since 1920.[18−20] Although parabens have been frequently blamed for their toxic properties, studies on the consequences and risks associated with the use of these compounds are still insufficient. We have previously reported the synthesis of paraben-based cyclotriphosphazene and cyclotetraphosphazene along with their effect on DNA as potential drug candidates.[21−23] Also, the results of our studies showed a direct effect of parabens on DNA that potentiates the synthesis of new genotoxic compounds.

Cyclotriphosphazene, one of the most important members of inorganic ring systems, is of interest to researchers because it can provide a stable and rigid platform for multifunctional molecular arrangements. From synthetic point of view, this platform can also easily give nucleophilic substitution reactions.[24,25] The reactivity of the cyclotriphosphazene allow to obtain different types of cyclotriphosphazene-based molecules with specific physical and chemical properties. Therefore, it provides different application fields for cyclotriphosphazene compounds. Studies related to the application areas of cyclotriphosphazene compounds have a wide place in the literature. Some of these applications are anticancer/antimicrobial agents, flame retardants, liquid crystals, and fluorescent chemosensors.[26−33] In particular, studies on the biological applications of cyclotriphosphazenes have become more important in recent years.[34−40,21−23]

For a designed anticancer compound to be valid in cancer research, it is essential that the compound has the ability to destroy DNA and is capable of killing rapidly abnormally dividing cells. The designed and synthesized molecules are expected to exhibit both the desired effect in the cancer cell and least side effects on living organisms at the same time. Although the research bears challenge, studies in this area continue rapidly and many researches arise to design new compounds as anticancer drugs. In this study, the novel series of paraben substituted dispirobino spermine derivative of cyclotriphosphazenes **2−6** were synthesized and their crystal structures examined for the first time. The compounds **2−6** have been fully characterized by MALDI−TOF mass analysis, ^{1}H, ^{31}P NMR spectroscopies and single crystal X-ray crystallography. Since the purity of the potential drug candidates is very important for biological activity studies, DSC measured melting points of the synthesized compounds. The sharp melt peaks in the DSC diagrams proved that the compounds are in high purity. The thermal stability of novel compounds **2−6** were also investigated. Conventional genotoxicity testing methods are laborious, time-consuming and expensive, which has led researchers to examine new methods. Biosensor-based analyzes, one of these methods, are an alternative way to study the interactions between the compound and DNA. For this purpose, an automated biosensor device has been used in the current study together with agarose gel electrophoresis to investigate possible DNA damages that are caused by presented compounds **2−6**. This biosensor device used in our study is based on real-time electrochemical profiling (REP) technology, an easy and fast scanning method. This means that the real-time amperometric measurements of an enzymatic signal (after DNA hybridization) during the flow of an enzyme substrate on a microfluidic channel integrated electrode array is feasible.

RESULTS AND DISCUSSION

Synthesis and Characterization of the Compounds 2−6. A new range of paraben-substituted dispirobinospermine derivative cyclotriphosphazene compounds **2−6** were successfully synthesized (Scheme 1).

In this context, spermine-bridged cyclotriphosphazene **1** was synthesized as a starting material according to the literature.[41] Reactions of compound **1** with methyl-, ethyl-, propyl-, butyl-, and benzyl paraben were then performed in the presence of sodium hydride and tetrahydrofuran to obtain full paraben-substituted dispirobinospermine derivative cyclotriphosphazenes **2−6**. All the synthesized compounds were purified by column chromatography and the identification of isolated compounds were carried out by MALDI−TOF mass spectrometry, DCS curves, and ^{1}H and ^{31}P NMR spectroscopies. The spectral data of compounds **1−6** are given in the Supporting Information (Figures S1−S31). In addition, the

https://dx.doi.org/10.1021/acs.inorgchem.9b03031
Inorg. Chem. XXXX, XXX, XXX−XXX

Table 1. ^{31}P NMR and Mass Parameters for Compounds 1−6[a]

	δ (^{31}P NMR) [ppm]				^{2}J(PP) [Hz]	mass	
compd	[PCl_2]	[$P(OR)_2$]	[$P(N{-}NH)_{spiro}$]	spin system	$^{2}J_{AX}$	$[M]^+$	$[M + H]^+$
1[b]	21.52	–	9.77	A_2X	40.44	751.44	–
2	–	8.79	19.64	AX_2	60.48	1677.54	–
3	–	8.71	19.68	AX_2	60.41	1789.22	–
4	–	8.73	19.75	AX_2	60.44	1901.27	–
5	–	8.70	19.72	AX_2	60.54	–	2014.30
6	–	8.66	19.68	AX_2	60.48	2286.95	–

[a]$CDCl_3$, [b]Reference 41.

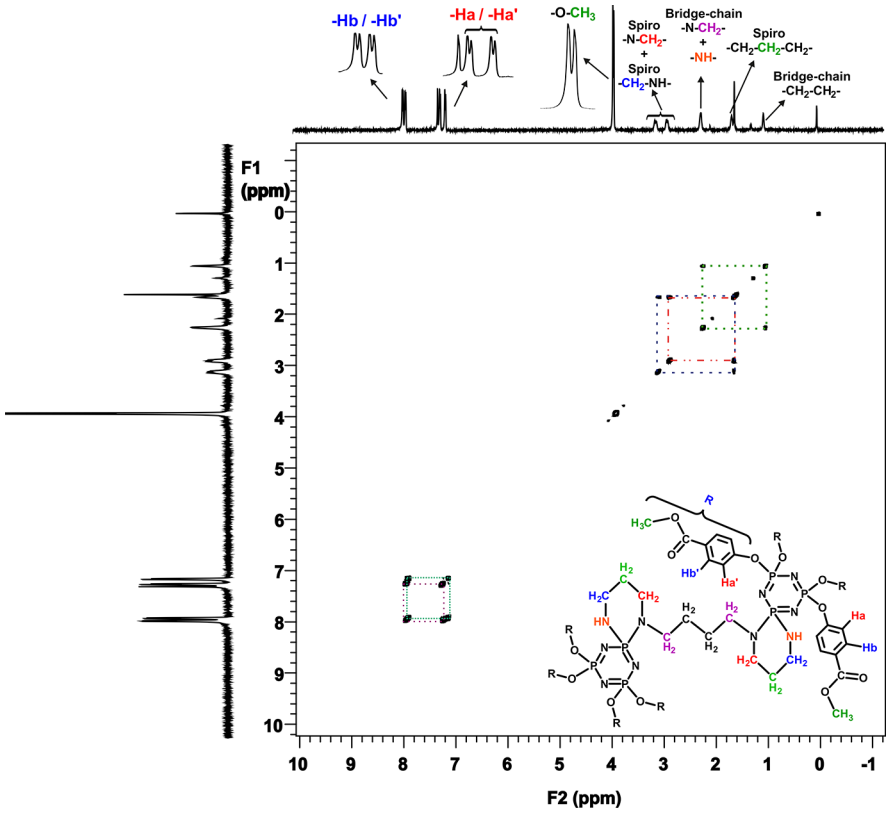

Figure 1. COSY ^{1}H NMR spectrum of the compound **2** in $CDCl_3$ solution.

crystal structures of compounds **2**−**6** were determined by single crystal X-ray diffraction. The structure analysis data include mass analysis results, ^{1}H NMR spectra and ^{31}P NMR chemical shifts. Phosphorus−phosphorus coupling constants for new compounds were also reported in the Experimental Section. Moreover, ^{31}P NMR data and the mass values for compounds **1**−**6** were summarized in Table 1. When the proton-decoupled ^{31}P NMR spectra of the compounds were examined, the spin systems of compounds **1**−**6** were observed as A_2X and AX_2. In general, in the ^{31}P NMR decoupled spectra of compounds **2**−**6**, chemical shift values of the [$P(OR)_2$] and *spiro* [$P(N{-}NH)_2$] groups were seen at around 8.66−8.79 ppm and 19.75−19.64 ppm, respectively (Table 1). The chemical signals were observed as one triplet for *spiro*[$P(N{-}NH)_2$] groups and as one doublet for [$P(OR)_2$] groups in the spectra. For example, the chemical shift of compound **6** ^{31}P NMR decoupled showed *spiro*[$P(N{-}NH)_2$] at 19.68 ppm ($^{2}J_{P-P}$ = 60.48 Hz) and [$P(OR)_2$] at 8.66 ppm ($^{2}J_{P-P}$ = 60.48 Hz). While the proton coupled ^{31}P NMR spectra of compounds **2**−**6** exhibited triplet peaks split into multiple peaks due to coupling with −N*H* proton, *spiro*-CH_2−NH−, and *spiro*-CH_2−N protons, the doublet peaks remained unchanged.

The ^{1}H NMR chemical shifts and coupling constants for compounds **2**−**6** were given in the Experimental Section. The paraben groups in the synthesized novel compounds face two different directions. Four of the eight paraben groups face toward the spermine bridged while the other four face to the phosphazene ring (out of the bridged). X-ray crystallography provided final confirmation of the structure. The ^{1}H NMR spectra illustrated that the paraben protons facing the bridged of the spermine and the paraben protons facing the phosphazene ring are close but different in chemical shifts. In order to support this, COSY ^{1}H NMR spectrum was recorded for compound **2** (Figure 1). Here, the COSY ^{1}H NMR spectrum of compound **2** showed that the aromatic and aliphatic protons of the paraben are differentiated (Figure 1).

Thermal Stabilities of Compounds 1−6. All of the compounds were stable in air at room temperature. The thermal stability of the starting material **1** and synthesized compounds **2**−**6** were investigated to determine the weight loss of a sample upon linearly increasing the temperature

https://dx.doi.org/10.1021/acs.inorgchem.9b03031
Inorg. Chem. XXXX, XXX, XXX−XXX

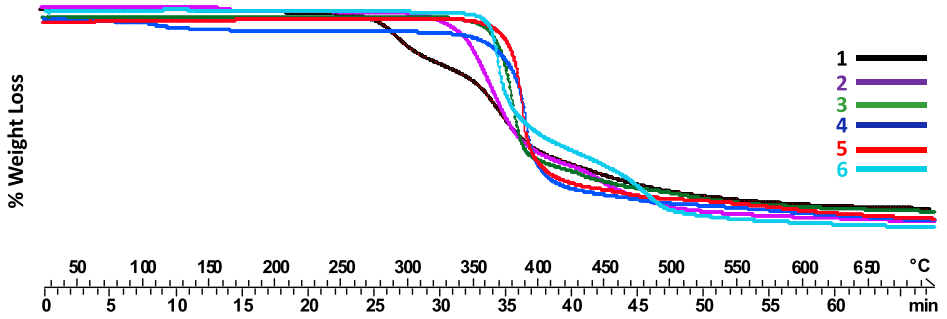

Figure 2. Thermogravimetric analysis of compounds **1**–**6**.

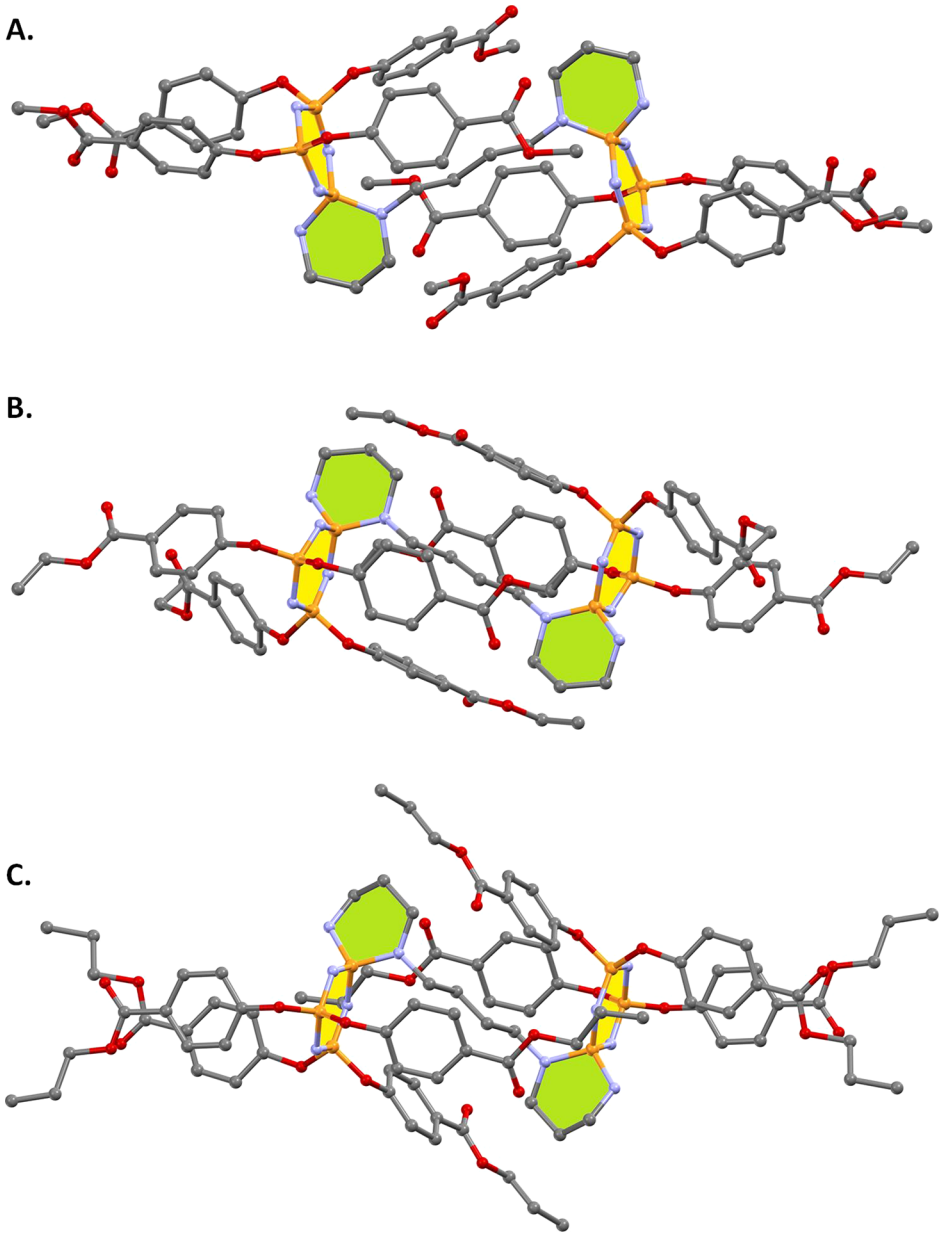

Figure 3. Ball–stick drawings of the molecular structures for compound **2** (a), **3** (b), and **3** (c) showing the corresponding N_3P_3 ring (light yellow colored) and P(N-spiro) (green colored). Gray, gold, blue, red and white colored atoms represent the C, P, N, O, and H atoms, respectively. All hydrogen atoms were omitted for clarity.

utilizing conventional thermogravimetric analysis (TGA) at a heating rate of 10 °C/min up to 700 °C under nitrogen flow. The thermal degradation analysis of the compounds was given in Figure 2. **1** has two-stage decomposition curve. Initial weight loss of 11.0% was observed at 296.4 °C, and the second one was detected at 377.8 °C with a weight loss of 33.4%. Here,

https://dx.doi.org/10.1021/acs.inorgchem.9b03031
Inorg. Chem. XXXX, XXX, XXX–XXX

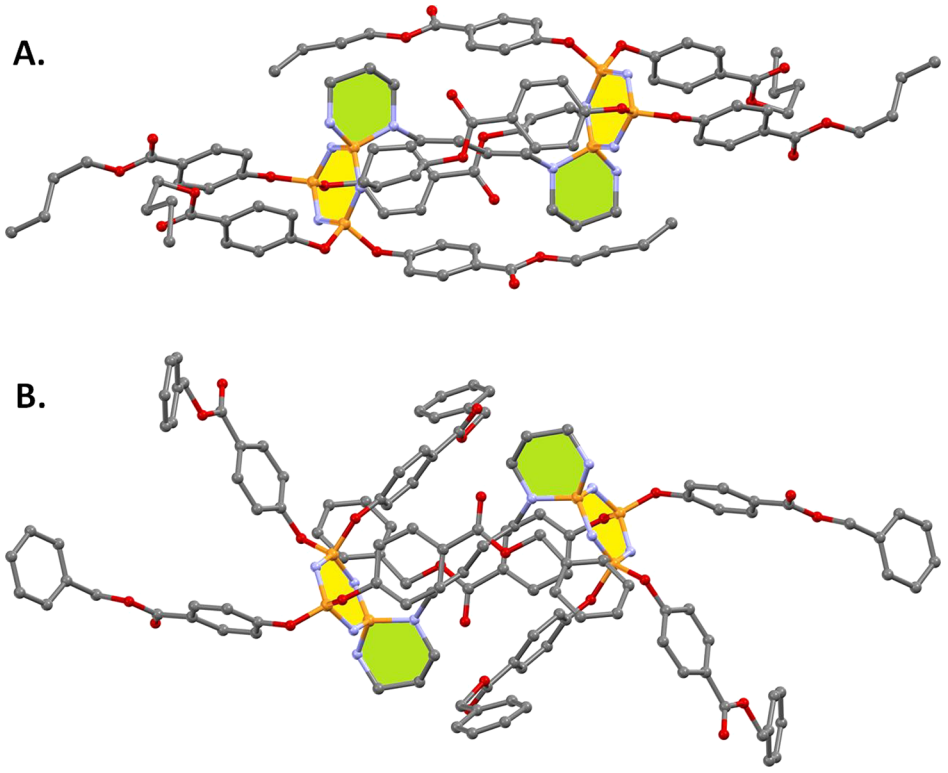

Figure 4. Ball−stick drawings of the molecular structures for compound **5** (a) and **6** (b). The N_3P_3 and P(N-spiro) rings are marked with different colors. All hydrogen atoms were omitted for clarity. Gray, gold, blue, red and white colored atoms represent the C, P, N, O, and H atoms, respectively.

54.9% of mass for **1** remained intact up to 377.8 °C. Also, compound **2** has two-step degradation at 357.8 °C with 45.3% weight loss and at 435.7 °C with 19.6% weight loss, respectively. Here, 35.1% of compound **2** stayed unspoiled. Compounds **3**, **4**, and **5** have one-step thermal disruption curves. The compounds were stable at 362.1, 357.9, and 361.3 °C and remaining amounts of compounds were 26.2%, 25.1%, and 24.6%, respectively. Compound **6** has two decomposition pathways: the first at 334.9 °C with 44.0% loss of mass and the second at 435.9 °C with 28.3%. Here, 27.6% of compound **6** stayed stable. The thermal stability of **1** was higher than that of compounds **2**−**6**. According to thermogravimetric analyses, all of the compounds have high thermal stability.

X-ray Crystallographic Characterizations of Compounds 2−6. The solid-state structures and geometries of compounds **2**−**6** were determined using single-crystal X-ray structural analysis. Crystallographic data and refinement details of the data collection for compounds **2**−**6** are given in Table S1. Compounds **3**, **4**, and **6** crystallize in the triclinic crystal system with a $P\bar{1}$ space group, whereas compounds **2** and **5** have the monoclinic crystal system with $P2_1/c$, respectively. The asymmetric unit of all compounds includes only one molecule and the cyclotriphosphazene rings are fully substituted with octamethyl-, ethyl-, propyl-, butyl-, and benzylparabens, as shown in ball−stick represantations in Figures 3 and 4. The selected bond and conformational parameters of compounds **2**-**6** in Tables S2−S6. The six-membered cyclotriphosphazene ring (N_3P_3) in each structure is nonplanar, and the total puckering amplitudes (Q_T) follow the order **2** > **3** > **6** > **5** > **4**. In cyclotriphosphazene rings (N_3P_3), the P−N bonds showed double-bond character, which are in the ranges 1.563(3)−1.596(3) Å for **2**, 1.5642(18)−1.6084(17) Å for **3**, 1.566(2)−1.599(2) Å for **4**, 1.554(6)−1.611(6) Å for **5**, and 1.5655(17)−1.6068(16) Å for **6**. The N−P−N bond angles in compounds are found in the range of 114.86(15)−118.99(16)° for **2**, 114.28(9)−119.72(9)° for **3**, 112.84(12)−119.07(12) for **4**, 114.5(3)−118.6(4) for **5**, and 114.68(8)−119.70(9) for **6**. On the other hand, P−N−P angles vary within the range of 119.78(11)−125.26(14)°, and are somewhat larger than those of the above-mentioned N−P−N angles. Analysis of previously reported crystallographic studies on spermine-bridged cyclophosphazene derivatives showed that a free rotation around single C−C bound in the flexible alkyl-chain could lead to the two conformations, which is identified as *syn* (CSD refcode: COPTUW01,[42] PAJVUS,[43] GUZPOG,[44] GUZPIA[44] or *anti* (CSD refcode: COPTUW,[41] BADJEW,[45] BADJIA,[45] CEGNEI,[46] CEGNIM,[46] GIFBAA[34]) conformations of the cyclophosphazene moiety with respect to each other. In all compounds, two cyclotriphosphazenes stand in *anti*-conformation to each other, possibly under the influence of crowded paraben groups.

DNA Interaction Analysis with Automated Electrochemical Biosensor of the Compounds 1−6. The investigation of synthesized compounds was performed using MiSens device, an automated electrochemical biosensor with sensitivity and fast response (Figure S32). DNA interaction assays with compounds **1**−**6** were carried out with an assay consists of several steps on microfluidic channel integrated biochip during flow. Cyclic voltammetry was used for measurements of electrochemical properties of the alkanethiol coating on the biochip surface (Figure S33). After the successful coating, the biotinylated surface DNA was captured on Neutravidin immobilized biochip surface. The complementary target sequence and biotinylated detection probe

https://dx.doi.org/10.1021/acs.inorgchem.9b03031
Inorg. Chem. XXXX, XXX, XXX−XXX

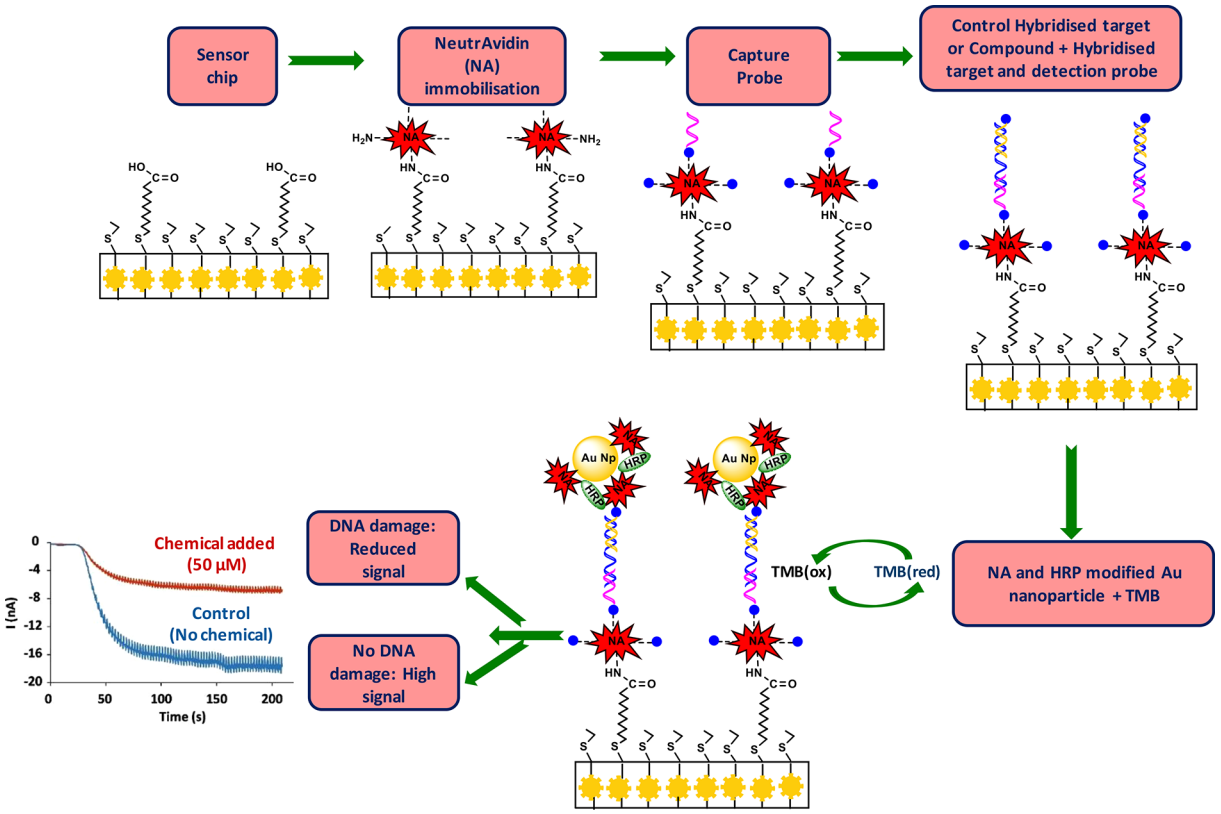

Figure 5. Schematics of the DNA damage test using MiSens device and the biochip. The amperometric raw data responses obtained from the biosensor assay have been shown in the figure for the control (no chemical added) and chemical added target and detection probe mixtures (TMB, 3,3′,5,5′-tetramethylbenzidine, HRP, horseradish peroxidase).

DNA were hybridized and then incubated with varying concentrations (0−50 μM) of compounds. This hybridized mixture was injected to the capture probe immobilized biochip surface to achieve the hybridization of the target to its complementary surface probe (capture probe). In the last step, enzyme HRP and Neutravidin-modified gold nanoparticles were injected to the biochip surface for binding via neutravidin and biotin interaction, and then an amperometric biosensor signal was measured during the substrate TMB injection (Figure 5).

The individual reactive **1** and the synthesized compounds **2**−**6** were tested by biosensor device. The hybridization activity results are shown Figure 6 indicated by remaining from interaction and interacting DNA. The hybridization activity of the reactive **1** has been compared to the compounds **2**−**6** in low concentrations (12.5 and 25 μM) and compounds **1** and **6** have shown the near activity reduction. When compounds **2**, **3**, and **4** have been compared with each other similar activity reduction were obtained, approximately 55% in 25 and 50 μM concentrations. At high concentration (50 μM), compounds **5** and **6** were considerably more reactive than the other synthesized compounds **2, 3** and **4**, resulted in 69% and 77% activity reduction, respectively. When the hybridization activity of the reactive **1** has been compared to compound **6**, it is acceptable to near value. The interaction of DNA and parabens with the synthesized new compounds were also compared. While parabens (methyl-, ethyl-, and propyl-) interact with DNA at a rate of 35−20%, it was observed that the bridged cyclotriphosphazene compounds **2**−**4** to which these parabens bind interact with DNA in approximately 50%. The DNA interactions of butyl- and benzylparaben and compounds **5** and **6** were compared, while the parabens showed a 28% effect at 50 μM concentration, compounds **5** and **6** showed at the same concentration 69% and 77% DNA interactions, respectively (Figure 6 and S34).

The Effects of Compounds on DNA Structure. The interaction of the synthesized compounds with pUC18 plasmid DNA was investigated using agarose gel electrophoresis. DNA can exist in three forms: supercoiled DNA (form I) as native plasmid, circular (form II), and linear (form III) when the helix strands are cut or damaged. All three forms of DNA can be differentiated on agarose gel as different bands regardless of their identical size: form I runs faster than form II and form III due to its compact rearrangement. In this study, the reaction of the compounds **1**−**6** with DNA were investigated in terms of converts from supercoil form of plasmid DNA (form I) to the open circular form (form II) or linearized DNA (form III). Also, DNA binding properties of the compounds were also examined using restriction enzymes and consequent observation of cleaved DNA forms on agarose gel. *Bam*HI, *Hin*dIII and *Eco*RI have been used as restriction enzymes and to cleave guanine−guanine (GG), adenine−adenine (AA) and guanine−adenine (GA) regions of the DNA, respectively.[47] If the compound has no effect on the DNA, it is expected that linear DNA (form III) as a single band will appear after the reaction with restriction enzymes.

For gels shown in Figure 7 line A, the first lane indicates untreated pUC18 plasmid DNA in TE buffer, the second lane represents untreated pUC18 plasmid DNA in % 0.1 DMSO as control, and lanes 3−5 are pUC18 plasmid DNA that was treated with increasing concentrations of the compounds **1**, **5**, and **6** (from 12.5 to 50 μM), respectively. In line B, the first

https://dx.doi.org/10.1021/acs.inorgchem.9b03031
Inorg. Chem. XXXX, XXX, XXX−XXX

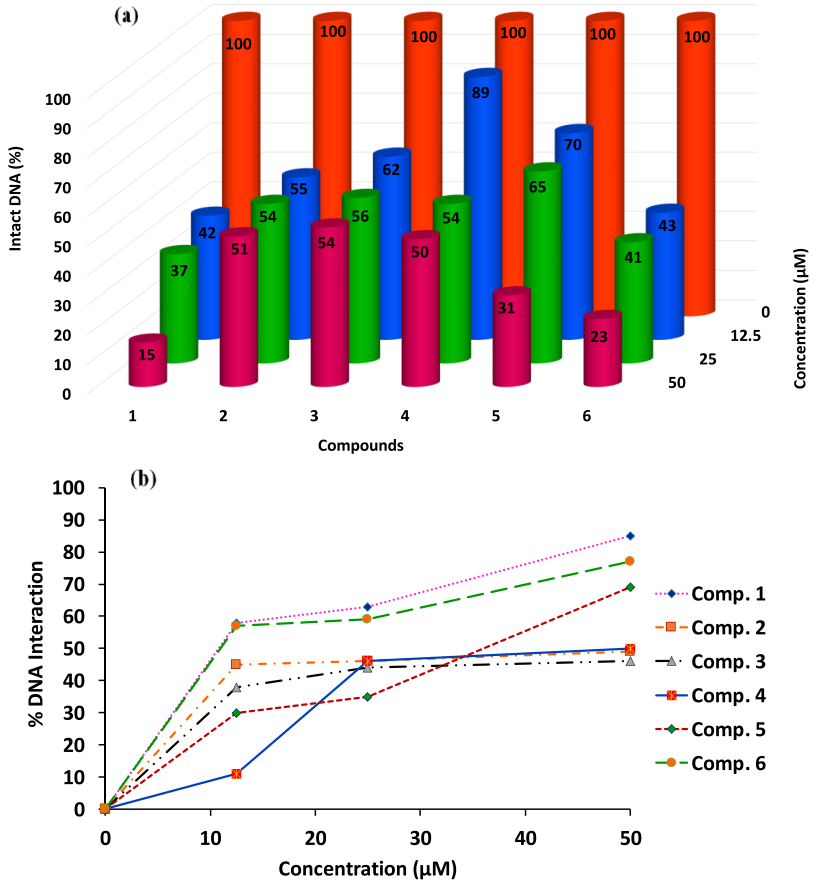

Figure 6. Amperometric responses were shown as percent relative hybridization responses in the figures, indicated by remaining from interaction (A) and interacting DNA (B). Compounds (0, 12.5, 25, and 50 μM) were incubated with DNA probes prior to the injection on to the biochip.

lane indicates *Bam*HI-enzyme-treated pUC18 plasmid DNA in 0.1% DMSO as control, lanes 2−4 contain *Bam*HI-enzyme-treated pUC18 plasmid DNA interacting with increasing concentrations of the compounds (from 12.5 to 50 μM), respectively. Lane 5 indicates *Eco*RI-enzyme-treated pUC18 plasmid DNA in 0.1% DMSO as control, lanes 6−8 represent *Eco*RI-enzyme-treated pUC18 plasmid DNA interacting with increasing concentrations of the compounds (from 12.5 to 50 μM), respectively. In line C, the first lane indicates *Hin*dIII-enzyme-treated pUC18 plasmid DNA in 0.1% DMSO as control, lanes 2−4 correspond to *Hin*dIII-enzyme-treated pUC18 plasmid DNA interacting with increasing concentrations of the compounds (from 12.5 to 50 μM), respectively. The bands at Figure 7 line represent the plasmid solution in the presence of TE or 0.1% DMSO as solvent control, impling that no change to the plasmid DNA form has been observed. Also, there are no considerable differences between the control and the compounds. However, as shown in Figure 7 line B, compound **1** has a significantly altered pUC18 plasmid DNA structure at all given concentrations (12.5−50 μM) in the reaction with the *Eco*RI restriction enzyme. In particular, at the highest concentration (50 μM), the formation of form III DNA could not be observed (Figure 7 line B lane 8). The results showed that the compound **1** has an effect on the plasmid DNA near the *Eco*RI restriction site. Likewise, compounds **5** and **6** showed the same effect on pUC18 plasmid DNA, but they clearly had a lower effect on the structure compared to compound **1**. Unlike compound **1**, *Eco*RI enzyme breaks DNA and produces form III DNA at 12.5 μM concentration of compounds **5**−**6**. For compounds **2**−**4** *Eco*RI, *Bam*HI, and *Hin*dIII enzymes break DNA, causing the appearance of form III; hence, it can be posited that compounds **2**−**4** have no detectable effect on plasmid DNA in electrophoresis (Figure S35). According to the data presented in Figure 7 line C and Figure S35 line C, *Hin*dIII could cut plasmid DNA. and this leads to formation of form III. On the basis of this observation, it can be safely concluded that all compounds have no effect on plasmid DNA near the *Hin*dIII restriction site.

EXPERIMENTAL SECTION

General Material and Methods. These are given in the Supporting Information.

Synthesis of Compound 1. Compound **1** was synthesized according to the literature,[41] and spectral data of compound **1** were given in the supporting file (Figures S1−S5).

Synthesis of Compound 2. Methyl 4-hydroxybenzoate (1.62 g, 10.64 mmol) and NaH (0.43 g, 10.64 mmol) were dissolved in 30 mL of dry THF under an argon atmosphere in a 100 mL three-necked round-bottomed flask. The reaction mixture was cooled in an ice bath, and compound **1** (1.00 g, 1.33 mmol) in 20 mL of dry THF was added dropwise over 30 min to a stirred solution under an argon atmosphere. The reaction mixture was refluxed in an oil bath with stirring for 5 days and followed on TLC silica gel plates using *n*-hexane:ethyl acetate (1:2) as eluent. The reaction mixture was filtered to remove the sodium chloride formed and the solvent removed under reduced pressure. The resulting white solid was subjected to column chromatography using *n*-hexane−ethyl acetate (1:2) as eluent. Compound **2**, isolated as white solid (1.80 g, 1.07 mmol, 81%; mp = 168.63 °C). Compound **2** was recrystallized from *n*-hexane:ethyl

https://dx.doi.org/10.1021/acs.inorgchem.9b03031
Inorg. Chem. XXXX, XXX, XXX−XXX

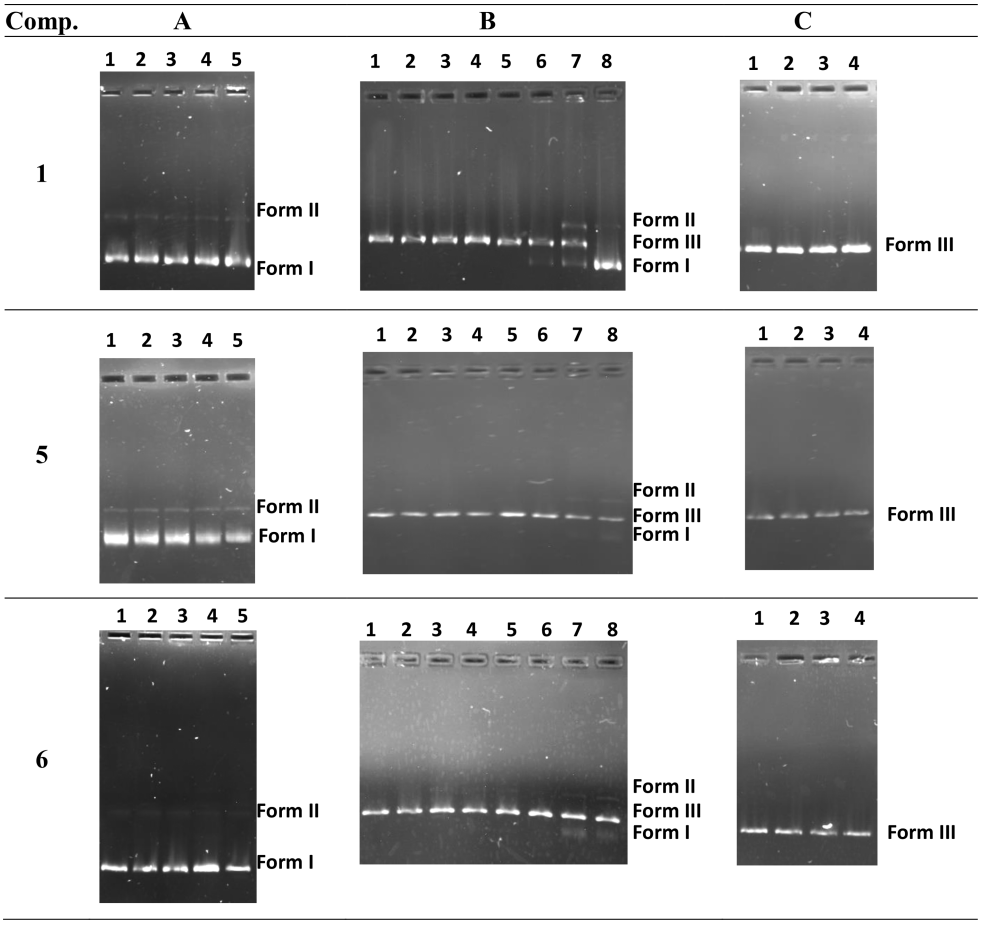

Figure 7. Agarose gel images of pUC18 plasmid DNA when incubated with different concentrations of compounds and *Eco*RI, *Hin*dIII and *Bam*HI digested mixtures of pUC18 plasmid DNA after treatment with various concentrations of compounds **1**, **5**, and **6**. Gels at the A line: lane 1, TE; lane 2, DMSO (0.1%); lanes 3−5, 12.5−25−50 μM. Gels at the B line: lane 1, *Bam*HI-treated pUC18 plasmid DNA in 0.1% DMSO; lanes 2−4, *Bam*HI-treated pUC18 plasmid DNA interacting with increasing concentrations of the compounds (12.5−50 μM); lane 5, *Eco*RI-treated pUC18 plasmid DNA in 0.1% DMSO; lanes 6−8, *Eco*RI-treated pUC18 plasmid DNA interacting with increasing concentrations of the compounds (from 12.5 to 50 μM). Gels at the C line: lane 1, *Hin*dIII-treated pUC18 plasmid DNA in 0.1% DMSO; lanes 2−4, *Hin*dIII-treated pUC18 plasmid DNA interacting with increasing concentrations of the compounds (12.5−50 μM).

acetate (1:2) and obtained as white crystals, which were suitable for single crystal X-ray crystallography. Spectral data of compound **2** follow. MS (MALDI−TOF) (DIT) *m*/*z* (%): calcd for ($C_{74}H_{78}N_{10}O_{24}P_6$), 1677.33; found, 1677.54 $[M]^+$ (Figure S6). ^{1}H NMR, $CDCl_3$, 298 K: δ ppm, δ_H 7.95 (d, $^3J_{HH}$ = 7.4 Hz, 8H) and 7.89 (d, $^3J_{HH}$ = 7.6 Hz, 8H) Hb/Hb′; 7.23 (d, $^3J_{HH}$ = 7.4 Hz, 8H) and 7.13 (d, $^3J_{HH}$ = 7.6 Hz, 8H) Ha/Ha′; 3.92 (s, 12H, $-OCH_3$); 3.90 (s, 12H, $-OCH_3$); 3.16−3.05 (m, 4H, *spiro*-CH_2−NH−); 2.94−2.84 (m, 4H, *spiro*-CH_2−N−); 2.30−2.19 (m, 4H + 2H, *bridge-chain*-CH_2−N− and −N*H*−); 1.68−1.61 (m, 4H, *spiro* $-CH_2-CH_2-CH_2-$); 1.07−1.00 (m, 4H, *bridge-chain*-$CH_2-CH_2-CH_2-$) (Figures S7 and S8). ^{31}P NMR decoupled to (202 MHz, $CDCl_3$, 298 K), *spiro*-$[P(N-NH)_2]$ δ = 19.64 ppm (1P, $^2J_{P-P}$ = 60.48 Hz); $[P(O)_2]$ δ = 8.79 ppm (2P, $^2J_{P-P}$ = 60.48 Hz). Spin system: AX_2 (Figures S9 and S10).

Synthesis of Compound 3. Ethyl 4-hydroxybenzoate, (1.77 g, 10.64 mmol) and NaH (0.43 g, 10.64 mmol) were dissolved in 30 mL of dry THF under an argon atmosphere in a 100 mL three-necked round-bottomed flask. The reaction mixture was cooled in an ice bath, and compound **1** (1.00 g, 1.33 mmol) in 20 mL of dry THF was added dropwise over 30 min to a stirred solution under an argon atmosphere. The reaction mixture was refluxed in an oil bath with stirring for 5 days and followed on TLC silica gel plates using *n*-hexane: ethyl acetate (6:5) as eluent. The reaction mixture was filtered to remove the sodium chloride formed and the solvent removed under reduced pressure. The resulting white solid was subjected to column chromatography using *n*-hexane−ethyl acetate (6:5) as eluent. Compound **3**, isolated as white solid (1.83 g, 1.02 mmol, 77%; mp = 126.34 °C). Compound **3** was recrystallized from *n*-hexane:ethyl acetate (6:5) and obtained as white crystals, which were suitable for single crystal X-ray crystallography. Spectral data of compound **3** follow. MS (MALDI−TOF) (DIT) *m*/*z* (%): calcd for ($C_{82}H_{94}N_{10}O_{24}P_6$), 1788.54; found, 1789.22 $[M]^+$ (Figure S11). ^{1}H NMR, $CDCl_3$, 298 K: δ ppm, δ_H 7.97 (d, $^3J_{HH}$ = 7.7 Hz, 8H) and 7.91 (d, $^3J_{HH}$ = 7.5 Hz, 8H) Hb/Hb′; 7.27 (d, $^3J_{HH}$ = 7.7 Hz, 8H) and 7.13 (d, $^3J_{HH}$ = 7.5 Hz, 8H) Ha/Ha′; 4.41−4.33 (m, 16H, $-OCH_2$); 3.16−3.03 (m, 4H, *spiro* $-CH_2$−NH−); 2.93−2.81 (m, 4H, *spiro*-CH_2−N−); 2.31−2.20 (m, 4H + 2H, *bridge-chain*-CH_2−N− and −N*H*−); 1.66−1.62 (m, 4H, *spiro* $-CH_2-CH_2-CH_2-$); 1.44−1.35 (m, 24H, $-CH_2-CH_3$);1.10−1.01 (m, 4H, *bridge-chain*-$CH_2-CH_2-CH_2-$) (Figures S12 and S13). ^{31}P NMR decoupled to (202 MHz, $CDCl_3$, 298 K), *spiro*-$[P(N-NH)_2]$ δ = 19.68 ppm (1P, $^2J_{P-P}$ = 60.41 Hz); $[P(O)_2]$ δ = 8.71 ppm (2P, $^2J_{P-P}$ = 60.41 Hz). Spin system: AX_2 (Figures S14 and S15).

Synthesis of Compound 4. Propyl 4-hydroxybenzoate, (1.92 g, 10.64 mmol) and NaH (0.43 g, 10.64 mmol) were dissolved in 30 mL of dry THF under an argon atmosphere in a 100 mL three-necked round-bottomed flask. The reaction mixture was cooled in an ice bath, and compound **1** (1.00 g, 1.33 mmol) in 20 mL of dry THF was added dropwise over 30 min to a stirred solution under an argon atmosphere. The reaction mixture was refluxed in an oil bath with stirring for 5 days and followed on TLC silica gel plates using *n*-hexane:ethyl acetate (2:1) as eluent. The reaction mixture was filtered

https://dx.doi.org/10.1021/acs.inorgchem.9b03031
Inorg. Chem. XXXX, XXX, XXX−XXX

to remove the sodium chloride formed and the solvent removed under reduced pressure. The resulting white solid was subjected to column chromatography using *n*-hexane:ethyl acetate (2:1) as eluent. Compound **4**, isolated as white solid (2.15 g, 1.13 mmol, 85%; mp = 99.37 °C). Compound **4** was recrystallized from *n*-hexane:ethyl acetate (2:1) and obtained as white crystals, which were suitable for single crystal X-ray crystallography. Spectral data of compound **4** follows. MS (MALDI−TOF) (DIT) *m*/*z* (%): calcd for ($C_{90}H_{110}N_{10}O_{24}P_6$), 1901.76; found, 1901.27 $[M]^+$ (Figure S16). ^{1}H NMR, $CDCl_3$, 298 K: δ ppm, δ_H 7.97 (d, $^3J_{HH}$ = 7.2 Hz, 8H) and 7.91 (d, $^3J_{HH}$ = 7.5 Hz, 8H) Hb/Hb′; 7.24 (d, $^3J_{HH}$ = 7.2 Hz, 8H) and 7.14 (d, $^3J_{HH}$ = 7.5 Hz, 8H) Ha/Ha′; 4.31−4.23 (m, 16H, $-OCH_2$); 3.16−3.03 (m, 4H, *spiro*-CH_2−NH−); 2.93−2.81 (m, 4H, *spiro*-CH_2−N−); 2.34−2.20 (m, 4H + 2H, *bridge-chain*-CH_2−N− and −NH−); 1.85−1.75 (m, 16H, *paraben*-CH_2−CH_3); 1.66−1.59 (m, 4H, *spiro*-CH_2−CH_2−CH_2−); 1.10−0.98 (m, 4H + 24H, *bridge chain* −CH_2−CH_2−CH_2− and −CH_2−CH_3) (Figures S17 and S18). ^{31}P NMR decoupled to (202 MHz, $CDCl_3$, 298 K), *spiro*-$[P(N{-}NH)_2]$ δ = 19.75 ppm (1P, $^2J_{P-P}$ = 60.44 Hz); $[P(O)_2]$ δ = 8.73 ppm (2P, $^2J_{P-P}$ = 60.44 Hz). Spin system: AX_2 (Figures S19 and S20).

Synthesis of Compound 5. Butyl 4-hydroxybenzoate, (2.07 g, 10.64 mmol) and NaH (0.43 g, 10.64 mmol) were dissolved in 30 mL of dry THF under an argon atmosphere in a 100 mL three-necked round-bottomed flask. The reaction mixture was cooled in an ice bath, and compound **1** (1.00 g, 1.33 mmol) in 20 mL of dry THF was added dropwise over 30 min to a stirred solution under an argon atmosphere. The reaction mixture was refluxed in an oil bath with stirring for 5 days and followed on TLC silica gel plates using *n*-hexane:ethyl acetate (3:1) as eluent. The reaction mixture was filtered to remove the sodium chloride formed and the solvent removed under reduced pressure. The resulting white solid was subjected to column chromatography using *n*-hexane−ethyl acetate (3:1) as eluent. Compound **5**, isolated as white solid (2.04 g, 1.01 mmol, 76%; mp = 88.90 °C). Compound **5** was recrystallized from *n*-hexane:ethyl acetate (3:1) and obtained as white crystals, which were suitable for single crystal X-ray crystallography. Spectral data of compound **5** follows. MS (MALDI−TOF) (DIT) *m*/*z* (%): calcd for ($C_{98}H_{126}N_{10}O_{24}P_6$), 2013.97; found, 2014.30 $[M + H]^+$. (Figure S21). ^{1}H NMR, $CDCl_3$, 298 K: δ ppm, δ_H 7.96 (d, $^3J_{HH}$ = 7.3 Hz, 8H) and 7.91 (d, $^3J_{HH}$ = 7.5 Hz, 8H) Hb/Hb′; 7.25 (d, $^3J_{HH}$ = 7.3 Hz, 8H) and 7.14 (d, $^3J_{HH}$ = 7.5 Hz, 8H) Ha/Ha′; 4.35−4.27 (m, 16H, $-OCH_2$); 3.16−3.03 (m, 4H, *spiro*-CH_2−NH−); 2.93−2.80 (m, 4H, *spiro*-CH_2−N−); 2.33−2.20 (m, 4H + 2H, *bridge-chain*-CH_2−N− and −NH−); 1.80−1.70 (m, 16H, *paraben*-CH_2−CH_2−); 1.66−1.59 (m, 4H, *spiro* −CH_2−CH_2−CH_2−); 1.53−1.42 (m, 16H, *paraben*-CH_2−CH_3); 1.11−1.04 (m, 4H, *bridge-chain*-CH_2−CH_2−CH_2−); 1.03−0.95 (m, 24H, −CH_2−CH_3) (Figures S22 and S23). ^{31}P NMR decoupled to (202 MHz, $CDCl_3$, 298 K), *spiro*-$[P(N{-}NH)_2]$ δ = 19.72 ppm (1P, $^2J_{P-P}$ = 60.54 Hz); $[P(O)_2]$ δ = 8.70 ppm (2P, $^2J_{P-P}$ = 60.54 Hz). Spin system: AX_2 (Figures S24 and S25).

Synthesis of Compound 6. Benzyl 4-hydroxybenzoate, (2.43 g, 10.64 mmol) and NaH (0.43 g, 10.64 mmol) were dissolved in 30 mL of dry THF under an argon atmosphere in a 100 mL three-necked round-bottomed flask. The reaction mixture was cooled in an ice bath, and compound **1** (1.00 g, 1.33 mmol) in 20 mL of dry THF was added dropwise over 30 min to a stirred solution under an argon atmosphere. The reaction mixture was refluxed in an oil bath with stirring for 5 days and followed on TLC silica gel plates using *n*-hexane:ethyl acetate (2:1) as eluent. The reaction mixture was filtered to remove the sodium chloride formed and the solvent removed under reduced pressure. The resulting white solid was subjected to column chromatography using *n*-hexane−ethyl acetate (2:1) as eluent. Compound **6**, isolated as white solid (2.42 g, 1.06 mmol, 80%; mp = 122.53 °C). Compound **6** was recrystallized from *n*-hexane:ethyl acetate (2:1) and obtained as white crystals, which were suitable for single crystal X-ray crystallography. Spectral data of compound **6** follows. MS (MALDI−TOF) (DIT) *m*/*z* (%): calcd for ($C_{122}H_{110}N_{10}O_{24}P_6$), 2286.11; found, 2286.95 $[M]^+$. (Figure S26). ^{1}H NMR, $CDCl_3$, 298 K: δ ppm, δ_H 7.98 (d, $^3J_{HH}$ = 7.6 Hz, 8H) and 7.93 (d, $^3J_{HH}$ = 7.8 Hz, 8H) Hb/Hb′; 7.48−7.30 (m, 45H, Ho/Hm/Hp); 7.22 (d, $^3J_{HH}$ = 7.6 Hz, 8H) and 7.12 (d, $^3J_{HH}$ = 7.8 Hz, 8H) Ha/Ha′; 5.33 (s, 8H, $-OCH_2$); 5.31 (s, 8H, $-OCH_2$); 3.08−2.94 (m, 4H, *spiro*-CH_2−NH−); 2.86−2.874 (m, 4H, *spiro*-CH_2−N−); 2.28−2.14 (m, 4H + 2H, *bridge-chain*-CH_2−N− and −NH−); 1.59−1.47 (m, 4H, *spiro*-CH_2−CH_2−CH_2−); 1.06−0.97 (m, 4H, *bridge-chain*-CH_2−CH_2−CH_2−) (Figures S27 and S28). ^{31}P NMR decoupled to (202 MHz, $CDCl_3$, 298 K), *spiro*-$[P(N{-}NH)_2]$ δ = 19.68 ppm (1P, $^2J_{P-P}$ = 60.48 Hz); $[P(O)_2]$ δ = 8.66 ppm (2P, $^2J_{P-P}$ = 60.48 Hz). Spin system: AX_2 (Figures S29 and S30).

CONCLUSION

In summary, this study is aimed to synthesize a series of cyclotriphosphazene compounds that are likely to be biologically active and to investigate synthesized compounds DNA interactions by two orthogonal methods. For this purpose, five new paraben-substituted dispirobinospermine (spermine-bridged) cyclotriphosphazene compounds **2**−**6** were successfully synthesized. In addition, the solid-state structures and geometries of all of the novel compounds were determined using single crystal X-ray structural analysis. While compounds **3**, **4**, and **6** crystallize in the triclinic crystal system with a $P\bar{1}$ space group, compounds **2** and **5** have a monoclinic crystal system with $P2_1/c$, respectively. Two different analysis methods were employed to investigate the DNA interaction properties of the final compounds. According to biosensor results, butyl- and benzylparaben-substituted spermine-bridged cyclotriphosphazene compounds **5** and **6** were significantly more reactive than the other paraben-substituted compounds **2**−**4**, resulting in 69% and 77% DNA interactions, respectively. Furthermore, studies with conventional analysis using plasmid DNA and electrophoresis have shown that compounds **1**, **5**, and **6** result in a change in the structure of plasmid DNA. The results of the biosensor analyze shows the effect of the compounds on the DNA strand rapidly, directly and quantitatively. It is worth noting here that studies on this device will help researchers to select the most likely drug candidates among many drug candidates.

ASSOCIATED CONTENT

Supporting Information

The Supporting Information is available free of charge at https://pubs.acs.org/doi/10.1021/acs.inorgchem.9b03031.

Experimental section, mass spectra, NMR spectra, DSC curves, crystal data parameters, biosensor and biochip, cyclic voltammetry, amperometric response, and electrophoretograms (PDF)

Accession Codes

CCDC 1955488−1955492 contain the supplementary crystallographic data for this paper. These data can be obtained free of charge via www.ccdc.cam.ac.uk/data_request/cif, or by emailing data_request@ccdc.cam.ac.uk, or by contacting The Cambridge Crystallographic Data Centre, 12 Union Road, Cambridge CB2 1EZ, UK; fax: +44 1223 336033.

AUTHOR INFORMATION

Corresponding Author

Elif Şenkuytu − *Department of Chemistry, Gebze Technical University, Gebze 41400, Turkey;* orcid.org/0000-0002-3579-8062; Phone: +90 2626053120; Email: senkuytu@gtu.edu.tr; Fax: +90 2626053101

https://dx.doi.org/10.1021/acs.inorgchem.9b03031
Inorg. Chem. XXXX, XXX, XXX−XXX

Authors

Perihan Kızılkaya − *Department of Chemistry, Gebze Technical University, Gebze 41400, Turkey; Faculty of Arts and Science, Department of Chemistry, Trakya University, Edirne 22020, Turkey*

Zehra Ölçer − *Department of Chemistry, Gebze Technical University, Gebze 41400, Turkey*

Uğur Pala − *Department of Chemistry, Gebze Technical University, Gebze 41400, Turkey*

Derya Davarcı − *Department of Chemistry, Gebze Technical University, Gebze 41400, Turkey*

Yunus Zorlu − *Department of Chemistry, Gebze Technical University, Gebze 41400, Turkey;* orcid.org/0000-0003-2811-1872

Huriye Erdoğan − *Department of Chemistry, Gebze Technical University, Gebze 41400, Turkey*

Gönül Yenilmez Çiftçi − *Department of Chemistry, Gebze Technical University, Gebze 41400, Turkey*

Complete contact information is available at: https://pubs.acs.org/10.1021/acs.inorgchem.9b03031

Notes

The authors declare no competing financial interest.

■ ACKNOWLEDGMENTS

This work was supported by a grant from the Scientific and Technical Research Council of Turkey (TUBITAK) (Grant No.: 118Z525). We would like to thank BILGEM-TUBITAK for their contribution to the manufacturing of biochip and detection platform.

■ REFERENCES

(1) Singh, D.; Narayanamoorthy, S.; Gamre, S.; Majumdar, A. G.; Goswami, M.; Gami, U.; Cherian, S.; Subramanian, M. Hydroxychavicol, a key ingredient of Piper betle induces bacterial cell death by DNA damage and inhibition of cell division. *Free Radical Biol. Med.* **2018**, *120*, 62−71.

(2) Choi, J.; Lee, J.; Kim, S. C.; You, S. G.; Lee, C. W.; Shin, J.; Park, Y. I. Glucuronorhamnoxylan from Capsosiphon fulvescens inhibits the growth of HT-29 human colon cancer cells in vitro and in vivo via induction of apoptotic cell death. *Int. J. Biol. Macromol.* **2019**, *124*, 1060−1068.

(3) Rescifina, A.; Chiacchio, U.; Corsaro, A.; Piperno, A.; Romeo, R. Isoxazolidinyl polycyclic aromatic hydrocarbons as DNA-intercalating antitumoragents. *Eur. J. Med. Chem.* **2011**, *46*, 129−136.

(4) Ni, Y.; Lin, D.; Kokot, S. Synchronous fluorescence and UV- vis spectrometric study of the competitive interaction of chlorpromazine hydrochloride and neutral red with DNA using chemometrics approaches. *Talanta* **2005**, *65*, 1295−1302.

(5) Ganeshpandian, M.; Ramakrishnan, S.; Palaniandavar, M.; Suresh, E.; Riyasdeen, A.; Akbarsha, M. A. Mixed ligand copper(II) complexes of 2,9-dimethyl-1,10-phenanthroline: Tridentate 3N primary ligands determine DNA binding and cleavage and cytotoxicity. *J. Inorg. Biochem.* **2014**, *140*, 202−212.

(6) Di Salvo, A. D.; Dugois, P.; Tandeo, D.; Peltekian, M.; Lin, P. K. T. Synthesis, cytotoxicity and DNA binding of oxoazabenzo[*de*]-anthracenes derivatives in colon cancer Caco-2 cells. *Eur. J. Med. Chem.* **2013**, *69*, 754−761.

(7) Esmaeili, C.; Heng, L. Y.; Chiang, C. P.; Rashid, Z. A.; Safitri, E.; Marugan, R. S. P. M. A DNA biosensor based on kappa-carrageenan-polypyrrole-gold nanoparticles composite for gender determination of Arowana fish (Scleropages formosus). *Sens. Actuators, B* **2017**, *242*, 616−624.

(8) Chen, X.; Yao, L.; Wang, Y.-C.; Chen, Q.; Deng, H.; Lin, Z.-Y.; Yang, H.-H. Novel electrochemical nanoswitch biosensor based on self-assembled pHsensitive continuous circular DNA. *Biosens. Bioelectron.* **2019**, *131*, 274−279.

(9) Yang, B.; Zhang, S.; Fang, X.; Kong, J. Double signal amplification strategy for ultrasensitive electrochemical biosensor based on nuclease and quantum dot-DNA nanocomposites in the detection of breast cancer 1 gene mutation. *Biosens. Bioelectron.* **2019**, *142*, 111544.

(10) Nowotarski, S. L.; Woster, P. M.; Casero, R. A. Polyamines and Cancer: Implications For Chemotherapy And Chemoprevention. *Expert Rev. Mol. Med.* **2013**, *15*, 1−28.

(11) Kwon, D. H.; Lu, C. D. Polyamines increase antibiotic susceptibility in Pseudomonas aeruginosa. *Antimicrob. Agents Chemother.* **2006**, *50*, 1623−1627.

(12) Perez-Cano, F. J.; Franch, A.; Castellote, C.; Castell, M. Immunomodulatory action of spermine and spermidine on NR8383 macrophage line in various culture conditions. *Cell. Immunol.* **2003**, *226*, 86−94.

(13) Darmostuk, M.; Jurášek, M.; Lengyel, K.; Zelenka, J.; Rumlová, M.; Drašar, P.; Ruml, T. Conjugation of Chlorins With Spermine Enhances Phototoxicity To Cancer Cells In Vitro. *J. Photochem. Photobiol., B* **2017**, *168*, 175−84.

(14) Valasinas, A.; Sarkar, A.; Reddy, V. K.; Marton, L. J.; Basu, H. S.; Frydman, B. Conformationally restricted analogues of 1N,14N-bisethylhomospermine (BE-4−4-4): syntheses and growth inhibitory effects on human prostate cancer cells. *J. Med. Chem.* **2001**, *44*, 390−403.

(15) Tarvirdipour, S.; Vasheghani-Farahani, E.; Soleimani, M.; Bardania, H. Functionalized Magnetic Dextran-Spermine Nanocarriers For Targeted Delivery Of Doxorubicin To Breast Cancer Cells. *Int. J. Pharm.* **2016**, *501*, 331−341.

(16) Pavlov, P.; Lin, P. K. T.; Rodilla, V. Cytotoxicity, DNA binding and localisation of novel bis-naphthalimidopropyl polyamine derivatives. *Chem.-Biol. Interact.* **2001**, *137*, 15−24.

(17) Delcros, J. G.; Tomasi, S.; Carrington, S.; Martin, B.; Renault, J.; Blagbrough, I. S.; Uriac, P. Effect of spermine conjugation on the cytotoxicity and cellular transport of acridine. *J. Med. Chem.* **2002**, *45*, 5098−5111.

(18) Andersen, F. A. Final amended report on the safety assessment of methylparaben, ethylparaben, propylparaben, isopropylparaben, butylparaben, isobutylparaben, and benzylparaben as used in cosmetic products. *Int. J. Toxicol.* **2008**, *27*, 1−82.

(19) Błędzka, D.; Gromadzińska, J.; Wąsowicz, W. Parabens from environmental studies to human health. *Environ. Int.* **2014**, *67*, 27−42.

(20) Haman, C.; Dauchy, X.; Rosin, C.; Munoz, J. F. Occurrence, fate and behavior of parabens in aquatic environments: a review. *Water Res.* **2015**, *68*, 1−11.

(21) Çiftci, G. Y.; Şenkuytu, E.; Incir, S. E.; Yuksel, F.; Olcer, Z.; Yildirim, T.; Kilic, A.; Uludag, Y. First paraben substituted cyclotetraphosphazene compounds and DNA interaction analysis with a new automated biosensor. *Biosens. Bioelectron.* **2016**, *80*, 331−338.

(22) Çiftci, G. Y.; Şenkuytu, E.; Incir, S. E.; Ecik, E. T.; Zorlu, Y.; Olcer, Z.; Uludag, Y. Characterization of paraben substituted cyclotriphosphazenes, and a DNA interaction study with a real-time electrochemical profiling based biosensor. *Microchim. Acta* **2017**, *184*, 2307−2315.

(23) Şenkuytu, E.; Yildirim, T.; Olcer, Z.; Uludag, Y.; Yenilmez Çiftci, G. DNA interaction analysis of fluorenylidene double bridged cyclotriphosphazene derivatives. *Inorg. Chim. Acta* **2018**, *477*, 219−226.

(24) Allen, C. W. Regio- and Stereochemical Control in Substitution Reactions of Cyclophosphazenes. *Chem. Rev.* **1991**, *91*, 119−135.

(25) Chandrasekhar, V.; Krıshnamurthy, S. S.; Woods, M. Metal Complexes of Amino(cyclophosphazenes). *Phosphorus Chemistry* **1981**, *171*, 481−485.

(26) Yu, J. Y.; Jun, Y. J.; Jang, S. H.; Lee, H. J.; Sohn, Y. S. Nanoparticulate platinum(II) anticancer drug: Synthesis and characterization of amphiphilic cyclotriphosphazene-platinum(II) conjugates. *J. Inorg. Biochem.* **2007**, *101*, 1931−1936.

https://dx.doi.org/10.1021/acs.inorgchem.9b03031
Inorg. Chem. XXXX, XXX, XXX−XXX

(27) Gorgulu, A. O.; Koran, K.; Ozen, F.; Tekin, S.; Sandal, S. Synthesis, structural characterization and anti-carcinogenic activity of new cyclotriphosphazenes containing dioxybiphenyl and chalcone groups. *J. Mol. Struct.* **2015**, *1087*, 1−10.
(28) Şenkuytu, E.; Eçik, E. T. New hexa-bodipy functionalized dendrimeric cyclotriphosphazene conjugates as highly selective and sensitive fluorescent chemosensor for Co^{2+} ions. *Spectrochim. Acta, Part A* **2018**, *198*, 232−238.
(29) Davarcı, D.; Tümay, S. O.; Şenkuytu, E.; Wörle, M.; Zorlu, Y. New one-dimensional mercury(II) coordination polymers built up from dispiro-dipyridyloxy-cyclotriphosphazene: Structural, thermal and UV-Vis absorption properties. *Polyhedron* **2019**, *161*, 104−110.
(30) Şenkuytu, E.; Eçik, E. T. Novel fully-BODIPY functionalized cyclotetraphosphazene photosensitizers having high singlet oxygen quantum yields. *Spectrochim. Acta, Part A* **2017**, *182*, 26−31.
(31) Cheng, J.; Wang, J.; Yang, S.; Zhang, Q.; Huo, S.; Zhang, Q.; Hu, Y.; Ding, G. Benzimidazolyl-substituted cyclotriphosphazene derivative as latent flame-retardant curing agent for one-component epoxy resin system with excellent comprehensive performance. *Composites, Part B* **2019**, *177*, 107440.
(32) Wang, D.; Feng, X.; Zhang, L.; Li, M.; Liu, M.; Tian, A.; Fu, S. Cyclotriphosphazene-bridged periodic mesoporous organosilica-integrated cellulose nanofiber anisotropic foam with highly flame-retardant and thermally insulating properties. *Chem. Eng. J.* **2019**, *375*, 121933.
(33) Jamain, Z.; Khairuddean, M.; Saidin, S. A. Synthesis and characterization of 1,4-phenylenediamine derivatives containing hydroxyl and cyclotriphosphazene as terminal group. *J. Mol. Struct.* **2019**, *1186*, 293−302.
(34) Ciftci, G. Y.; Ecik, E. T.; Yildirim, T.; Bilgin, K.; Şenkuytu, E.; Yuksel, F.; Uludag, Y.; Kilic, A. Synthesis and characterization of new cyclotriphosphazene Compounds. *Tetrahedron* **2013**, *69*, 1454−1461.
(35) Yıldırım, T.; Bilgin, K.; Çiftçi, G. Y.; Eçik, E. T.; Şenkuytu, E.; Uludağ, Y.; Tomak, L.; Kılıç, A. Synthesis, cytotoxicity and apoptosis of cyclotriphosphazene compounds as anti-cancer agents. *Eur. J. Med. Chem.* **2012**, *52*, 213−220.
(36) Akbaş, H.; Karadağ, A.; Aydın, A.; Destegül, A.; Kılıç, Z. Synthesis, structural and thermal properties of the hexapyrrolidino-cyclotriphosphazenes-based protic molten salts:Antiproliferative effects against HT29, HeLa, and C6 cancer cell lines. *J. Mol. Liq.* **2017**, *230*, 482−495.
(37) Siwy, M.; Sęk, D.; Kaczmarczyk, B.; Jaroszewicz, I.; Nasulewicz, A.; Pelczynska, M.; Nevozhay, D.; Opolski, A. Synthesis and in Vitro Antileukemic Activity of Some New 1,3-(Oxytetraethylenoxy)-cyclotriphosphazene Derivatives. *J. Med. Chem.* **2006**, *49*, 806−810.
(38) Asmafiliz, N.; Berberoğlu, İ.; Özgür, M.; Kılıç, Z.; Kayalak, H.; Açık, L.; Türk, M.; Hökelek, T. Phosphorus-nitrogen compounds: Part 46. The reactions of $N_3P_3Cl_6$ with bidentate and monodentate ligands: The syntheses, structural characterizations, antimicrobial and cytotoxic activities, and DNA interactions of (N/N)-spirocyclotriphosphazenes with 4-chlorobenzyl pendant arm. *Inorg. Chim. Acta* **2019**, *495*, 118949.
(39) Song, S.-C.; Lee, S. B.; Lee, B. H.; Ha, H.-W.; Lee, K.-T.; Sohn, Y. S. Synthesis and antitumor activity of novel thermosensitive platinum(II)-cyclotriphosphazene conjugates. *J. Controlled Release* **2003**, *90*, 303−311.
(40) Chelike, D. K.; Alagumalai, A.; Acharya, J.; Kumar, P.; Sarkar, K.; Thangavelu, S. A. G.; Chandrasekhar, V. Functionalized iron oxide nanoparticles conjugate of multi-anchored Schiffs base inorganic heterocyclic pendant groups: Cytotoxicity studies. *Appl. Surf. Sci.* **2020**, *501*, 143963.
(41) Labarre, J. F.; Guerch, G.; Sournies, F.; Lahana, R.; Enjalbert, R.; Galy, J. An answer to the spiro versus ansa diemma in cyclophosphazenes: Part IV. Reaction of spermidine and spermine on $N_3P_3Cl_6$. *J. Mol. Struct.* **1984**, *116*, 75−88.
(42) Yenilmez Ciftci, G. Synthesis and characterization of per-substituted spermine-bridged cyclophosphazene derivatives: the first example of syn/anti conformational polymorphism in a bridged cyclophosphazene. *Inorg. Chem. Commun.* **2004**, *7*, 1258−1260.
(43) Coles, S. J.; Davies, D. B.; Hursthouse, M. B.; Kilic, A.; Mayer, T. A.; Shaw, R. A.; Yenilmez Ciftci, G. Structural investigations of phosphorus-nitrogen compounds. 6. Relationships between molecular parameters in per-X-substituted bridged spermine derivatives and basicity constants RaR of substituents. *Acta Crystallogr., Sect. B: Struct. Sci.* **2004**, *60*, 739−747.
(44) Besli, S.; Coles, S. J.; Davies, D. B.; Eaton, R. J.; Hursthouse, M. B.; Kilic, A.; Shaw, R. A.; Yenilmez Ciftci, G.; Yesilot, S. Anomalous NMR Behavior of Meso Compounds with Remote Stereogenic Centers on Addition of Chiral Shift Reagent or Chiral Solvating Agent. *J. Am. Chem. Soc.* **2003**, *125*, 4943−4950.
(45) Coles, S. J.; Davies, D. B.; Eaton, R. J.; Hursthouse, M. B.; Kilic, A.; Mayer, T. A.; Shaw, R. A.; Yenilmez, G. Chiral configurations of spermine-bridged cyclotriphosphazatrienes. *J. Chem. Soc., Dalton Trans.* **2002**, 365−370.
(46) Coles, S. J.; Davies, D. B.; Eaton, R. J.; Kilic, A.; Shaw, R. A.; Ciftci, G. Y. Structural and stereogenic properties of spiro- and ansa-substituted1,3-propanedioxy derivatives of a spermine-bridgedcyclotriphosphazene. *Polyhedron* **2006**, *25*, 953−962.
(47) Yıldırım, T.; Şenkuytu, E.; Ergene, E.; Bilgin, K.; Uludağ, Y.; Çiftçi, G. Y. Biological Activity of New Cyclophosphazene Derivatives Including Fluorenylidene-Bridged Cyclophosphazenes. *Chem. Select* **2018**, *3*, 9933−9939.

https://dx.doi.org/10.1021/acs.inorgchem.9b03031
Inorg. Chem. XXXX, XXX, XXX−XXX